Association Between ICP Pulse Waveform Morphology and ICP B Waves

Magdalena Kasprowicz, Marvin Bergsneider, Marek Czosnyka, and Xiao Hu

Abstract The study aimed to investigate changes in the shape of ICP pulses associated with different patterns of the ICP slow waves (0.5–2.0 cycles/min) during ICP overnight monitoring in hydrocephalus. Four patterns of ICP slow waves were characterized in 44 overnight ICP recordings (no waves – NW, slow symmetrical waves – SW, slow asymmetrical waves – AS, slow waves with plateau phase – PW). The morphological clustering and analysis of ICP pulse (MOCAIP) algorithm was utilized to calculate a set of metrics describing ICP pulse morphology based on the location of three subpeaks in an ICP pulse: systolic peak (P_1), tidal peak (P_2) and dicrotic peak (P_3). Step-wise discriminant analysis was applied to select the most characteristic morphological features to distinguish between different ICP slow waves. Based on relative changes in variability of amplitudes of P_2 and P_3 we were able to distinguish between the combined groups NW + SW and AS + PW ($p < 0.000001$). The AS pattern can be differentiated from PW based on respective changes in the mean curvature of P_2 and P_3 ($p < 0.000001$); however, none of the MOCAIP feature separates between NW and SW. The investigation of ICP pulse morphology associated with different ICP B waves may provide additional information for analysing recordings of overnight ICP.

M. Kasprowicz
Neural Systems and Dynamics Laboratory, Department of Neurosurgery, The David Geffen School of Medicine, University of California, NPI 18-265, 10833, Le Conte Avenue, Los Angeles, CA 90095, USA

Institute of Biomedical Engineering and Instrumentation, Wroclaw University of Technology, Wroclaw, Poland and Academic Neurosurgical Unit, Addenbrooke's Hospital, Cambridge, UK

M. Bergsneider and X. Hu (✉)
Neural Systems and Dynamics Laboratory, Department of Neurosurgery, The David Geffen School of Medicine, University of California, NPI 18-265, 10833, Le Conte Avenue, Los Angeles, CA 90095, USA

Biomedical Engineering Graduate Program, Henry Samueli School of Engineering and Applied Science, University of California, Los Angeles, CA, USA
e-mail: xhu@mednet.ucla.edu

M. Czosnyka
Academic Neurosurgical Unit, Addenbrooke's Hospital, Cambridge, UK

Keywords Intracranial pressure • Waveform analysis • Hydrocephalus

Introduction

Previously, we have studied the feasibility of distinguishing ICP B waves (0.5–2.0 cycles/min) of any shape and strength from flat ICP recordings based on ICP pulse morphology and mean value of ICP [9]. The present study was designed to investigate whether ICP B waves of different shapes are associated with different ICP pulse waveform morphology. Mean values of ICP were excluded from this study in order to solely investigate changes in ICP pulse shape. We hypothesised that ICP waveform morphology reflects cerebrovascular changes [10]. Given that ICP B waves are thought to arise from vasomotor instability and ICP, waveform morphology associated with B waves should be unique. The study aimed to investigate whether or not the shape of the ICP pulse waveforms changes in association with the ICP B wave occurrence and to identify the discriminating power of metrics describing ICP pulse waveform morphology to differentiate between different patterns of ICP B wave activities in overnight monitoring of hydrocephalus.

Materials and Methods

A total number of 276 episodes of four clearly distinctive ICP slow wave activities (Fig. 1a–d) were selected from retrospectively analysed pre-shunt operation, overnight intracranial pressure (ICP) recordings performed in 44 patients (18 female and 26 male; mean age: 68 ± 17 years, range 32–94 years) hospitalised at the UCLA Adult Hydrocephalus Centre. The preliminary diagnosis (based on brain scans and clinical picture) for all patients was hydrocephalus. One hundred and thirty-one selections of flat ICP patterns containing no episodes of slow waves (NW), 74 selections of symmetrical slow waves (SW), 45 selections of asymmetrical slow

M.U. Schuhmann and M. Czosnyka (eds.), *Intracranial Pressure and Brain Monitoring XIV*,
Acta Neurochirurgica Supplementum, Vol. 114, DOI: 10.1007/978-3-7091-0956-4_6, © Springer-Verlag/Wien 2012

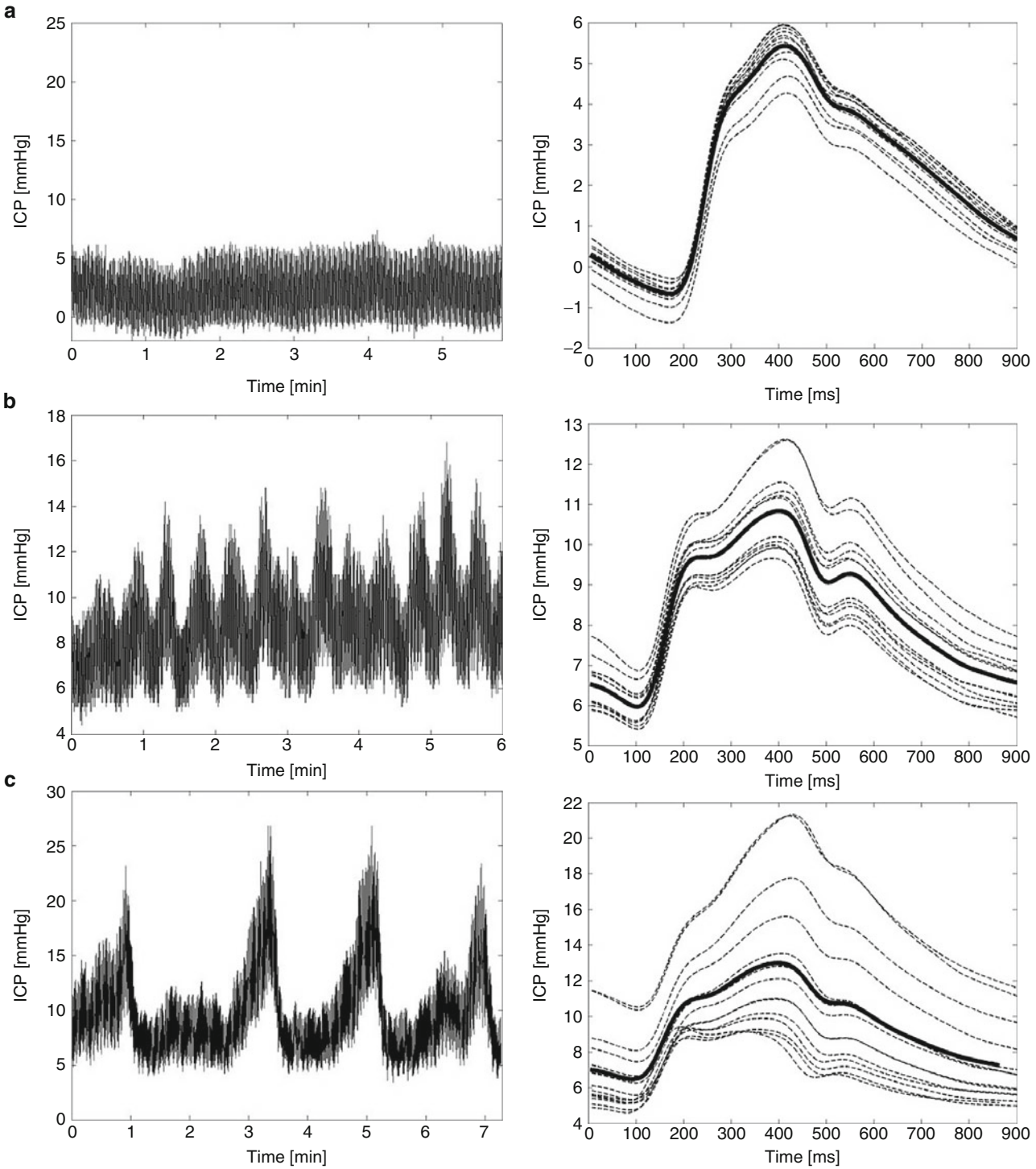

Fig. 1 Four patterns of intracranial pressure (*ICP*) oscillations and corresponding dominant ICP pulses: (**a**) NW – no episodes of ICP B waves, (**b**) SW – symmetrical ICP B waves, (**c**) AS – asymmetrical ICP B waves, (**d**) PW – slow ICP B with plateau phase. Each dominant pulse was extracted from 30 s of data

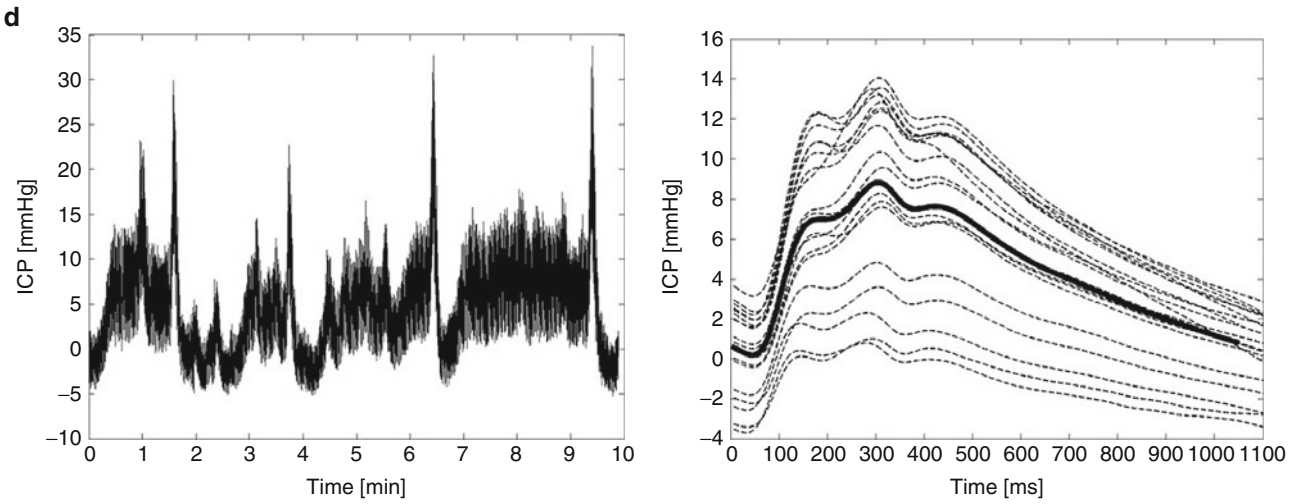

Fig. 1 (continued)

waves (AS) and 26 selections of slow waves with plateau phase (PW) were included into this study. Mean duration of selection was 9 min 58 s ± 4 min 15 s. An ICP intraparenchymal microsensor (Codman and Schurtleff, Raynaud, MA, USA) was inserted into the right frontal lobe. Simultaneous recordings of ICP and ECG signals were performed using either a PowerLab™ SP-16 acquisition system (ADInstruments, Colorado Springs, CO, USA) connected to the analogue outputs of the Codman ICP Express Box and the GE bedside monitor or the BedMaster™ system, which acquire data from bedside monitors. A different sampling rate was used by the acquisition systems: PowerLab™ – 400 Hz and BedMaster™ – 240 Hz. An insertion of the ICP sensor and data acquisition were approved by the local IRB committee and informed consent was obtained from each patient or from their family member.

The morphological clustering and analysis of ICP pulse (MOCAIP) algorithm was utilized to measure the set of ICP pulse metrics based on the location of sub-peaks in an ICP pulse: systolic peak (P_1), tidal peak (P_2) and dicrotic peak (P_3). Details of this algorithm were precisely described in another publication [8]. The set of 10 ICP pulse metrics was calculated to describe the morphology of ICP pulsation: amplitudes of pulse peaks (dP_1, dP_2, dP_3), latency (L_T) between the peak of the QRS complex of ECG and the corresponding onset of the ICP pulse, latencies between the onset of ICP pulse and the location of three peaks (L_1, L_2, L_3) and curvatures of the three sub-waves of ICP pulse wave ($Curv_1$, $Curv_2$, $Curv_3$). The average of the MOCAIP features quantitatively estimates the ICP pulse wave shape, although it ignores the changes during slow wave occurrence (Fig. 1). Therefore, besides mean values of 10 MOCAIP metrics, we also calculated their standard deviations (S.D.). Hence, a total number of metrics analysed increased to 20 (Table 1).

Statistical Methods

With regard to statistical analysis, the forward step-wise discriminant analysis (DA) [12] was used to investigate which features are the most significantly altered by ICP B wave occurrence. At each step of analysis 20 MOCAIP metrics were reviewed and evaluated to determine which one will contribute most to the discrimination between four patterns of ICP B wave activity (NW, SW, AS and PW). The step-wise procedure was controlled by F to enter value (set at 4.0) and minimum tolerance value ($1 - R^2$ set at 0.01). We repeated the analysis 44 times; in every run the samples from one patient were excluded and the selections from the remaining 43 patients were used to build the discriminant model. Only the metrics that were selected most often (more than 22 times) were included in the final analysis. The significance of the discriminant functions obtained was tested based on a multivariate F value (Wilks' lambda statistics). Standardised beta coefficients were utilised for estimation of the unique power of discrimination of the variables. To identify between which of the groups the respective function discriminates we looked at the means of canonical variables.

Results

Mean values and standard deviations of ICP pulse metrics along with the number indicating how many times a particular metric was chosen by DA were summarised in Table 2. Nine out of 20 ICP pulse metrics were selected more than 22 times. Eight of them (highlighted in grey in Table 2) were accepted (based on the p value for the F statistic <0.05) into the final model (Wilks' lambda: 0.31, $F = 16.2$, $p < 0.0001$).

Table 1 Intracranial pressure (ICP) pulse wave metrics

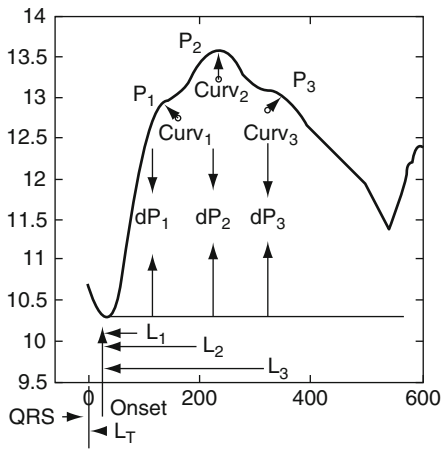

MOCAIP Metric Group	Mean	S.D.
Pulse wave amplitudes	dP_1, dP_2, dP_3	$SDdP_1$, $SDdP_2$, $SDdP_3$
Pulse waves latencies	L_T, L_1, L_2, L_3	SDL_T, SDL_1, SDL_2, SDL_3
Pulse curvatures	$Curv_1$, $Curv_2$, $Curv_3$	$SDCurv_1$, $SDCurv_2$, $SDCurv_3$

Table 2 Mean (±SD) and standard deviation (±SD) of the ICP pulse metrics for four patterns of ICP fluctuations

		No DA select	NW ± SD (N=131)	SW ± SD (N=74)	AS ± SD (N=45)	PW ± SD (N=26)
dP_1 (mmHg)	Mean	0	4.08 ± 1.56	4.66 ± 1.84	5.93 ± 2.29	5.98 ± 2.55
	SD	10	0.25 ± 0.14	0.41 ± 0.23	0.89 ± 0.57	1.00 ± 0.80
dP_2 (mmHg)	Mean	0	5.16 ± 2.08	6.40 ± 2.46	8.42 ± 3.75	9.03 ± 3.56
	SD	44	0.46 ± 0.22	0.92 ± 0.48	2.13 ± 1.21	2.02 ± 1.11
dP_3 (mmHg)	Mean	39	3.71 ± 1.77	4.77 ± 1.87	6.17 ± 2.64	6.85 ± 3.08
	SD	0	0.46 ± 0.23	0.84 ± 0.44	1.73 ± 0.93	1.66 ± 0.95
L_T	Mean	0	108.6 ± 32.5	109.1 ± 30.0	105.1 ± 35.2	102.7 ± 30.4
	SD	0	2.6 ± 1.5	3.8 ± 6.5	3.8 ± 2.0	3.4 ± 1.7
L_1	Mean	0	100.6 ± 13.4	101.2 ± 11.8	103.4 ± 9.9	107.0 ± 13.9
	SD	31	4.6 ± 2.7	5.4 ± 3.4	6.9 ± 3.8	6.7 ± 3.1
L_2	Mean	1	233.6 ± 27.7	236.9 ± 35.3	249.8 ± 21.6	241.6 ± 25.8
	SD	1	6.6 ± 4.3	6.7 ± 3.5	10.2 ± 6.0	5.7 ± 2.1
L_3	Mean	35	370.9 ± 30.4	363.7 ± 43.5	380.4 ± 28.8	356.6 ± 31.2
	SD	43	6.1 ± 3.0	6.5 ± 3.3	10.0 ± 3.8	8.1 ± 4.1
$Curv_1^{-3}$ (1/mmHg)	Mean	1	4.5 ± 6.8	4.0 ± 5.8	4.1 ± 6.7	2.7 ± 7.0
	SD	41	1.3 ± 1.2	2.2 ± 3.0	2.4 ± 2.7	1.1 ± 1.1
$Curv_2^{-3}$ (1/mmHg)	Mean	26	5.8 ± 5.0	8.9 ± 6.6	8.2 ± 5.6	10.0 ± 6.9
	SD	23	0.8 ± 0.7	1.7 ± 1.6	3.2 ± 2.9	2.0 ± 1.5
$Curv_3^{-3}$ (1/mmHg)	Mean	25	3.5 ± 3.4	3.5 ± 3.3	4.3 ± 3.3	2.1 ± 2.3
	SD	0	0.6 ± 0.4	0.8 ± 0.6	1.4 ± 1.1	0.9 ± 1.2

Eight metrics (*highlighted in grey*) were accepted (based on the p value for the F statistic <0.05) into the final discriminant model

Three discriminant functions (the maximal possible number) were statistically significant. The first function (Function 1, $p<0.000001$) differentiates between two groups: combined PW and AS vs combined SW and NW. It explains 83.6% of discriminating power while the second and the third ones account for 16.4% of total power. The standardized coefficients for the two variables $SDdP_2$ and $SDdP_3$, demonstrated the greatest values; therefore, their contributions to discrimination between PW + AS vs SW + NW are the most significant (Eq. 1).

$$2.3SDdP_2 - 1.3SDdP_3 - 0.4\mathrm{SDCurv}_1 + 0.3\mathrm{SDL}_1 + 0.3\mathrm{SDL}_3 + 0.2\mathrm{Curv}_2 - 0.2\mathrm{SDCurv}_2 - 0.1\mathrm{Curv}_3 \quad (1)$$

The Function 2 ($p<0.000001$) discriminates between PW and AS groups mostly based on inverse changes in mean Curv_2 and Curv_3 (Eq. 2).

$$1.2Curv_2 - 1.1Curv_3 - 0.6\mathrm{SDCurv}_2 - 0.4\mathrm{SDL}_3 + 0.2\mathrm{SDL}_1 + 0.2\mathrm{SDCurv}_1 + 0.2\mathrm{SDdP}_3 + 0.0\mathrm{SDdP}_2 \quad (2)$$

The Function 3 ($p<0.002$) separates between PW and SW and the variables SDdP_2 and SDdP_3 have the biggest impact on this discrimination (Eq. 3)

$$2.1SDdP_2 - 2.0SDdP_3 - 0.7\mathrm{SDCurv}_2 - 0.7\mathrm{SDCurv}_1 + 0.3\mathrm{Curv}_3 + 0.2\mathrm{SDL}_1 - 0.1\mathrm{Curv}_2 + 0.1\mathrm{SDL}_3 \quad (3)$$

To visualise how the two functions discriminate between groups the individual scores for the two functions (Function 1 vs Function 2) were plotted on Fig. 2.

The variation of amplitudes of peaks P_2 and P_3 contributes to the distinction between NW + SW vs AS + PW (Fig. 3). Mean values of SDdP_2 and SDdP_3 evolve from NW to PW when different ICP patterns were compared (Fig. 3a). The discriminating power, however, was attributed to the relative changes between SDdP_2 and SDdP_3: profound variations in dP_2 prevailed over the changes in dP_3 during AS and PW, but the range of variation in amplitudes of these two peaks was similar during SW and NW (Fig. 3a). The highest discriminating power to distinguish between PW and AS was ascribed to the mean curvatures of the two peaks P_2 and P_3. A more rounded sub-wave of P_2 along with a less sharp sub-wave of P_3 seems to be typical for PW (Fig. 3b). We could not find any significant combination of MOCAIP features to distinguish between SW and NW.

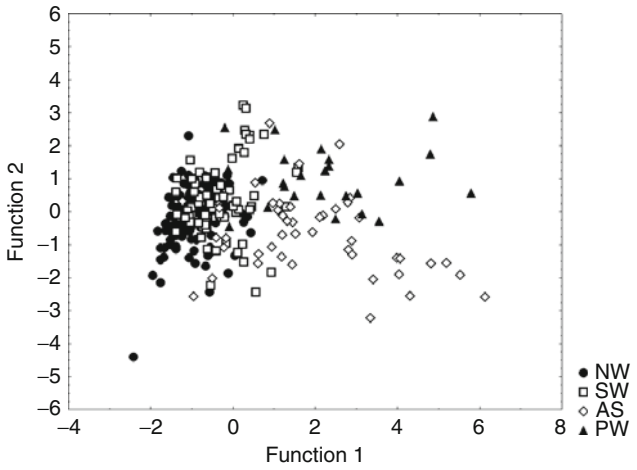

Fig. 2 Scatter plot of the canonical scores from the discriminant analysis of (•) no ICP B waves, (□) symmetrical ICP B waves, (◊) asymmetrical ICP B waves, (▲) slow ICP B with plateau phase PW

Discussion

Based solely upon ICP pulse morphological features (mean ICP values were not taken into account in this study), we were able to demonstrate that different subtypes of ICP B waves are indeed associated with different shaped ICP pulsations and a different range of alterations of MOCAIP metrics. Our finding suggests then that AS and PW might be physiologically distinct from SW and NW. Moreover, AS and PW may also be physiologically different.

The changes in ICP pulse morphological features reflect acute changes in intracranial conditions and changes in the cerebral haemodynamics [1, 2]. The origin of the three peaks in ICP pulse waveform has not yet been established. The P_2 component is thought to be dependent upon intracranial compliance [6] whereas pulsations of major arteries and choroid plexus may contribute to the P_1 component [2, 13]. Miller noted that venous hypertension from jugular venous or sagittal sinus occlusion causes an increase in the terminal portion of the ICP pulse wave, which suggests the venous pressure dependency of P_3 [2, 13]. Recent study in TBI patients showed that the amplitude of ICP was mostly affected by changes in the pulsatility of the cerebral blood volume (CBV), whereas in patients with NPH, who underwent an infusion study, amplitude was more dependent upon mean ICP, which was increased during the test in a controllable manner [3]. In the case of ICP B waves, both factors (mean ICP and increased pulsatility of CBV) play a significant role. As the ICP slow waves are most probably vasogenic in origin, they may be dependent on cerebral blood volume pulsatility [4, 7]. Moreover, the compliance in NPH patients is usually reduced owing to underlying pathological conditions, which may amplify an increase in mean ICP during ICP B waves and provoke proportional changes in ICP pulse amplitude [11, 15].

In our study the distinguishing power was mostly related to variation in the amplitudes of two peaks: P_2 and P_3, which may reflect more reduced intracranial compliance and increased venous pressure because of an elevation in ICP during AW and PW ICP B waves compared with during NW and SW. It was suggested by recent studies [5] that an increased amplitude of ICP pulsation may have predictive value for selecting shunt responders. It was also discussed in an early work [14], where a five-category classification of B wave was proposed, that only the asymmetrical B wave has a predictive value with regard to outcome after shunting. Therefore,

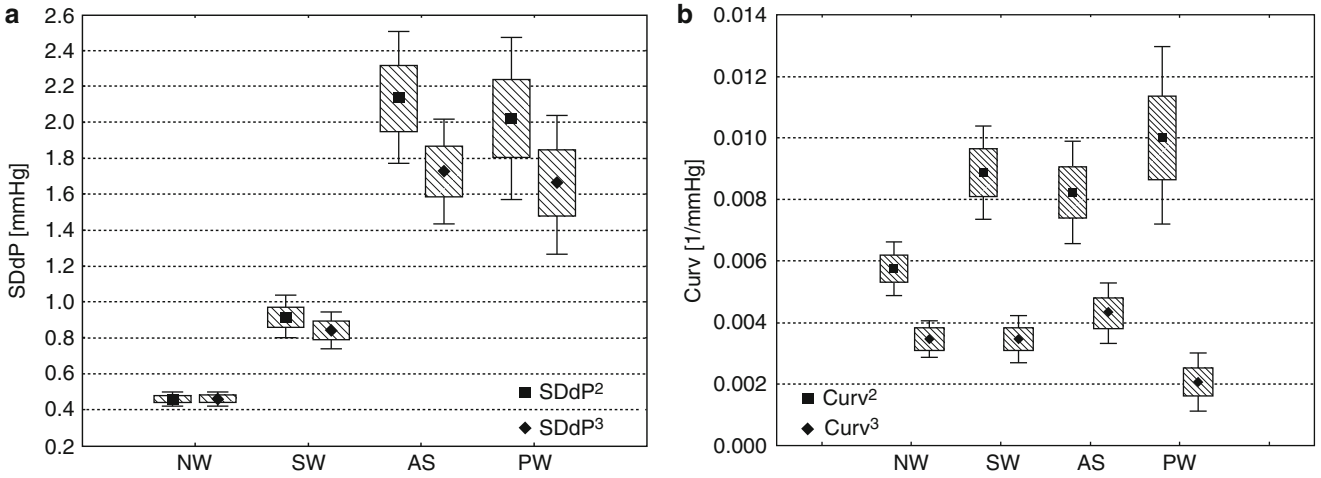

Fig. 3 Mean ± SE (*box*) ±95% confidence interval (whiskers) of (**a**) $SDdP_2$ and $SDdP_3$ and (**b**) $Curv_2$ and $Curv_3$ for four patterns of ICP oscillation: NW – no episodes of ICP B waves, SW – symmetrical ICP B waves, AS – asymmetrical ICP B waves, PW – slow ICP B with the plateau phase

we think that joint analysis of both ICP pulse wave amplitudes and ICP B waves (AS and PW in particular) performed in hydrocephalic patients undergoing overnight monitoring might be ideal for overnight ICP analysis. Further study is needed to establish the usefulness of such a joint approach.

Conclusion

Subtypes of ICP slow wave are associated with different configurations of morphological features describing ICP pulse waves, which may suggest that they are physiologically distinct.

Acknowledgement The present work is partially supported by NINDS R21 awards NS055998, NS055045 and NS059797 and R01 awards NS054881 and NS066008. MK is supported by the Foundation for Polish Science.

Conflict of interest statement We declare that we have no conflict of interest.

References

1. Avezaat CJ, van Eijndhoven JH, Wyper DJ (1979) Cerebrospinal fluid pulse pressure and intracranial volume-pressure relationships. J Neurol Neurosurg Psychiatry 42:687–700
2. Cardoso ER, Rowan JO, Galbraith S (1983) Analysis of the cerebrospinal fluid pulse wave in intracranial pressure. J Neurosurg 59:817–821
3. Carrera E, Kim DJ, Castellani G, Zweifel C, Czosnyka Z, Kasprowicz M, Smielewski P, Pickard J, Czosnyka M (2009) What shapes pulse amplitude of intracranial pressure? J Neurotrauma 27:317–324
4. Droste DW, Krauss JK, Berger W, Schuler E, Brown MM (1994) Rhythmic oscillations with a wavelength of 0.5-2 min in transcranial Doppler recordings. Acta Neurol Scand 90:99–104
5. Eide PK, Brean A (2006) Intracranial pulse pressure amplitude levels determined during preoperative assessment of subjects with possible idiopathic normal pressure hydrocephalus. Acta Neurochir (Wien) 148:1151–1156; discussion 1156
6. Germon K (1988) Interpretation of ICP pulse waves to determine intracerebral compliance. J Neurosci Nurs 20:344–351
7. Haubrich C, Czosnyka Z, Lavinio A, Smielewski P, Diehl RR, Pickard JD, Czosnyka M (2007) Is there a direct link between cerebrovascular activity and cerebrospinal fluid pressure-volume compensation? Stroke 38:2677–2680
8. Hu X, Xu P, Scalzo F, Vespa P, Bergsneider M (2009) Morphological clustering and analysis of continuous intracranial pressure. IEEE Trans Biomed Eng 56:696–705
9. Kasprowicz M, Asgari S, Bergsneider M, Czosnyka M, Hamilton R, Hu X (2010) Pattern recognition of overnight intracranial pressure slow waves using morphological features of intracranial pressure pulse. J Neurosci Methods 190:310–318
10. Kirkness CJ, Mitchell PH, Burr RL, March KS, Newell DW (2000) Intracranial pressure waveform analysis: clinical and research implications. J Neurosci Nurs 32:271–277
11. Marmarou A, Shulman K, LaMorgese J (1975) Compartmental analysis of compliance and outflow resistance of the cerebrospinal fluid system. J Neurosurg 43:523–534
12. McNitt-Gray MF, Huang HK, Sayre JW (1995) Feature selection in the pattern classification problem of digital chest radiograph segmentation. IEEE Trans Med Imaging 14:537–547
13. Miller JD, Peeler DF, Pattisapu J, Parent AD (1987) Supratentorial pressures. Part I: differential intracranial pressures. Neurol Res 9:193–197
14. Raftopoulos C, Deleval J, Chaskis C, Leonard A, Cantraine F, Desmyttere F, Clarysse S, Brotchi J (1994) Cognitive recovery in idiopathic normal pressure hydrocephalus: a prospective study. Neurosurgery 35:397–404; discussion 404–395
15. Szewczykowski J, Sliwka S, Kunicki A, Dytko P, Korsak-Sliwka J (1977) A fast method of estimating the elastance of the intracranial system. J Neurosurg 47:19–26